Cyclodextrin Protects Podocytes in Diabetic Kidney Disease

Sandra Merscher-Gomez,[1] Johanna Guzman,[1,2] Christopher E. Pedigo,[1] Markku Lehto,[3,4] Robier Aguillon-Prada,[1,2] Armando Mendez,[2] Mariann I. Lassenius,[3,4] Carol Forsblom,[3,4] TaeHyun Yoo,[1] Rodrigo Villarreal,[1,2] Dony Maiguel,[2] Kevin Johnson,[2] Ronald Goldberg,[2] Viji Nair,[5] Ann Randolph,[5] Matthias Kretzler,[5] Robert G. Nelson,[6] George W. Burke III,[2,7] Per-Henrik Groop,[3,4] Alessia Fornoni,[1,2] and the FinnDiane Study Group

Diabetic kidney disease (DKD) remains the most common cause of end-stage kidney disease despite multifactorial intervention. We demonstrated that increased cholesterol in association with downregulation of ATP-binding cassette transporter *ABCA1* occurs in normal human podocytes exposed to the sera of patients with type 1 diabetes and albuminuria (DKD^+) when compared with diabetic patients with normoalbuminuria (DKD^-) and similar duration of diabetes and lipid profile. Glomerular downregulation of *ABCA1* was confirmed in biopsies from patients with early DKD (n = 70) when compared with normal living donors (n = 32). Induction of cholesterol efflux with cyclodextrin (CD) but not inhibition of cholesterol synthesis with simvastatin prevented podocyte injury observed in vitro after exposure to patient sera. Subcutaneous administration of CD to diabetic BTBR (black and tan, brachiuric) *ob/ob* mice was safe and reduced albuminuria, mesangial expansion, kidney weight, and cortical cholesterol content. This was followed by an improvement of fasting insulin, blood glucose, body weight, and glucose tolerance in vivo and improved glucose-stimulated insulin release in human islets in vitro. Our data suggest that impaired reverse cholesterol transport characterizes clinical and experimental DKD and negatively influences podocyte function. Treatment with CD is safe and effective in preserving podocyte function in vitro and in vivo and may improve the metabolic control of diabetes.
***Diabetes* 62:3817–3827, 2013**

Diabetic kidney disease (DKD) is responsible for nearly half of the incidents of end-stage kidney disease in the U.S. (1), yet our current understanding of the pathophysiological processes responsible for DKD has led to limited improvements in patient outcomes. Multifactorial intervention reduces the rate of progression of DKD but does not prevent end-stage kidney disease in type 1 (T1D) or type 2 diabetes (T2D) (2,3). A key factor for this translation gap is the current lack of adequate mechanistic insight into DKD in humans.

The kidney glomerulus is a highly specialized structure that ensures the selective ultrafiltration of plasma so that essential proteins are retained in the blood (4). Podocytes are glomerular epithelial cells that contribute to the glomerular filtration barrier through a tight regulation of actin cytoskeleton remodeling (4). Currently, the diagnosis of DKD relies on the detection of microalbuminuria (5). However, a growing body of evidence suggests that key histological lesions precede the development of albuminuria (6,7); among them, decreased podocyte number (podocytopenia) has been described as an independent predictor of DKD progression (8–12). Although we have previously shown that podocyte insulin resistance and susceptibility to apoptosis is already present at the time of onset of microalbuminuria in experimental models of DKD, the cause of podocyte injury in early DKD remains unknown (13).

We used a previously established cell-based assay in which differentiated human podocytes are exposed to 4% patient sera for 24 h (14) to identify new pathways and targets in DKD. Podocytes exposed to the sera of patients with DKD showed increased cholesterol accumulation in association with downregulation of ATP-binding cassette transporter 1 (*ABCA1*) expression that was independent of circulating cholesterol.

ABCA1 is a major regulator of cellular cholesterol homeostasis by mediating efflux to lipid-poor apolipoprotein acceptors in the bloodstream (15). *ABCA1* genetic variants are strongly associated with the risk of coronary artery disease (16). Furthermore, the capacity of patient sera to induce ABCA1-mediated cholesterol efflux in macrophages is impaired in patients with T2D and incipient or overt nephropathy (17). Excessive cholesterol accumulation has been described in glomeruli of rodent models of T1D and T2D (18–20) and may contribute to DKD development and progression. Finally, inactivating mutations of *ABCA1* result in Tangier disease, which causes premature atherosclerosis and proteinuria (21).

Although interventions that increase *ABCA1* expression (such as liver X receptor agonists) may be beneficial in DKD, they have a relatively high incidence of adverse events (22) as well as intrinsic lipogenic effects (23). We used β-cyclodextrins, cyclic oligosaccharides consisting of seven β(1-4)-glucopyranose rings, to remove cholesterol from differentiated human podocytes in vitro and from diabetic animals in vivo. The exact mechanism by which cyclodextrins (CDs) remove cholesterol from cells is not completely understood, but the formation of cholesterol/

From the [1]Division of Nephrology and Hypertension, Department of Medicine, University of Miami Miller School of Medicine, Miami, Florida; the [2]Diabetes Research Institute, University of Miami Miller School of Medicine, Miami, Florida; the [3]Folkhälsan Institute of Genetics, Folkhälsan Research Center, Biomedicum Helsinki, Helsinki, Finland; the [4]Division of Nephrology, Department of Medicine, Helsinki University Central Hospital, Helsinki, Finland; the [5]University of Michigan, Ann Arbor, Michigan; the [6]National Institute of Diabetes and Digestive and Kidney Diseases, Phoenix, Arizona; and the [7]Department of Surgery, University of Miami, Miami, Florida.
Corresponding author: Alessia Fornoni, afornoni@med.miami.edu.
Received 12 March 2013 and accepted 14 June 2013.
DOI: 10.2337/db13-0399
This article contains Supplementary Data online at http://diabetes.diabetesjournals.org/lookup/suppl/doi:10.2337/db13-0399/-/DC1.
S.M.-G. and J.G. share co-first authorship.

See accompanying commentary, p. 3661.

CD inclusion complexes at the membrane surface plays an important role in this process (24).

We hypothesized that 2-hydroxypropyl-β-cyclodextrin, which was recently approved by the U.S. Food and Drug Administration (FDA) for the cure of Niemann-Pick disorder (25,26), would be an effective way to sequester cholesterol and to protect podocytes from cholesterol-dependent damage in DKD in vivo and in vitro.

RESEARCH DESIGN AND METHODS

Patient sera and kidney biopsies. Serum samples were obtained from 10 healthy controls and 20 patients with T1D from the Finnish Diabetic Nephropathy Study (FinnDiane). T1D was defined as onset of diabetes before 40 years of age and permanent insulin treatment initiated within 1 year of diagnosis. Urinary albumin excretion rate (AER) was defined as normal AER (<30 mg/24 h), microalbuminuria (≥30, <300 mg/24 h), and macroalbuminuria (≥300 mg/24 h). Fasting glucose values were measured using a Hemocue device (Hemocue, Helsinki, Finland). Serum lipids were determined with a Konelab analyzer (Thermo Scientific, Vantaa, Finland). Other biochemical analyses were performed in an accredited hospital laboratory (HUSLAB, Helsinki, Finland). For glomerular mRNA expression profiles, kidney biopsy specimens were procured from 70 Southwestern American Indians after obtaining informed consent. Human renal biopsies from pretransplant, healthy living donors (n = 32) and membranous nephropathy (n = 21) and focal segmental glomerulosclerosis (n = 18) patients were obtained from the European Renal cDNA Bank.

Illumina array platform analysis and Affymetrix GeneChip analysis. For Illumina array platform analysis, four pools of sera were prepared per patient group, healthy controls, DKD^-, and DKD^+, by combining sera from two to three patients. Podocytes were treated with 4% of the pooled sera (four C, four DKD^-, and four DKD^+ pools) for 24 h. More detailed protocol information and results are available at http://www.ncbi.nlm.nih.gov/geo/query/acc.cgi?acc=GSE46900.

For glomerular mRNA expression profiles of *ABCA1*, *HMG-CoA*, *LDLR*, *SREBP1*, and *SREBP2*, kidney biopsy specimens were procured from 70 Southwestern American Indians enrolled in a randomized, placebo-controlled, clinical trial to evaluate the renoprotective efficacy of losartan in T2D (clinicaltrials.gov, NCT00340678) after obtaining informed consent. Human renal biopsies from pretransplant, healthy living donors (n = 32) and membranous nephropathy (n = 21) and focal segmental glomerulosclerosis (n = 18) patients were obtained from the European Renal cDNA Bank according to the guidelines of local ethics committees. Biopsy tissue specimens were microdissected as previously described (27–29). Glomerular gene expression profiling was performed using Human Genome U133A and U133plus2 Affymetrix GeneChip arrays (27,29). Raw image files were normalized and annotated. Log2-transformed datasets were batch corrected using Combat (30) from Genepattern. Differential regulation analysis between control and disease groups was performed using significance analysis of microarray (SAM) as implemented in the Mev software suite (31,32). Genes passing a false discovery rate (FDR) correction (qvalue) for multiple testing <5% were considered significantly regulated.

Human podocyte culture. Human podocytes were cultured and differentiated in RPMI culture medium containing 10% FBS and 1% penicillin/streptomycin as previously described (33). In brief, immortalized normal human podocytes were propagated at 33°C and then thermoshifted for differentiation for 14 days at 37°C. Terminally differentiated podocytes were serum and insulin starved in 0.1% FBS (insulin experiments) or 0.2% FBS for all other experiments. When patient sera were used, starved cells were exposed to 4% patient sera in FBS-free culture medium for 24 h. For insulin treatment experiments, 100 nmol insulin was added to the culture medium for 15 min after exposure to patient sera. For CD or statin treatment experiments, serum-starved human podocytes were pretreated for 1 h with 5 mmol/L methyl-β-cyclodextrin (Sigma-Aldrich) or simvastatin (1 μmol/L; Sigma-Aldrich).

Immunofluorescence staining. Cells cultured in chamber slides were fixed with 4% paraformaldehyde for 30 min at 37°C and permeabilized with 0.1% Triton X-100, followed by exposure to mouse antiphosphorylated caveolin (pY14; BD Biosciences), anti-active RhoA (New East Biosciences), or antivimentin (Sigma-Aldrich) antibodies. Fluorescence detection was performed using Alexa Fluor secondary antibodies (Invitrogen). For cholesterol determination, filipin (Sigma-Aldrich) staining was performed as previously described (34). F-actin was visualized by rhodamine phalloidin (Invitrogen). Two hundred consecutive cells per condition were studied. Slides were prepared with DAPI-enriched mounting media (Vectashield) and analyzed by confocal microscopy.

Apoptosis analysis. Apoptosis was assessed using the Caspase-3/CPP32 Colorimetric Assay Kit (Biovision) according to the manufacturer's description. Caspase 3 activity was normalized to cell number and expressed as fold change to controls.

Determination of cholesterol content and cholesterol efflux assay. Esterified cholesterol was determined as difference between total and free cholesterol using an enzymatic assay and normalized to cell protein content (35). The cellular content of lipid droplets was determined using Oil Red O (ORO). Cells were fixed and permeabilized as described above, washed in PBS and in 60% isopropanol, incubated in ORO (0.5% ORO in isopropanol, 1:3 diluted) for 15 min at room temperature, and counterstained with hematoxylin for 1 min. The fraction of ORO-positive cells over 200 consecutive cells was calculated by bright field microscopy. To measure cholesterol efflux from differentiated human podocytes, a previously described method (36) was used with some modifications. Differentiated human podocytes were labeled with 2 μCi/mL [^{3}H]cholesterol in medium with 2% FBS for 16 h, and the cells were washed with PBS and then incubated in RPMI containing 0.5% patient sera for 6 h. Four independent experiments were performed, and each sample was run in duplicate or triplicate. Cholesterol efflux to medium containing serum was expressed as percent of total cell cholesterol as previously described (36,37).

Western blotting and Luminex. Cell lysate collection and Western blotting was performed as previously described (14). The following primary antibodies were used: rabbit polyclonal anti-MyD88 (Cell Signaling), rabbit polyclonal antiphosphorylated (Y_{473}) or antitotal AKT (Cell Signaling), mouse monoclonal anti-RhoA (Santa Cruz Biotechnology), or mouse monoclonal anti-Gapdh (6C5; Calbiochem) antibody. Secondary anti-mouse IgG-HRP or and anti-rabbit IgG-HRP conjugate (Promega) were used. Image acquisition was performed using the chemiluminescent imager SRX-101A (Konica Minolta Medical Imaging, Ramsey, NJ), and band densitometry was analyzed using ImageJ software (National Institutes of Health [NIH]). Alternatively, phosphorylated/total AKT was quantified using Luminex technology as previously reported (38).

Quantitative real-time PCR. Podocyte RNA was extracted using the RNAeasy Mini Kit (Qiagen). Reverse transcription was performed using the high-capacity cDNA reverse transcriptase kit (Applied Biosystems) according to the manufacturer's protocols. Quantitative real-time PCR (RT-PCR) was performed in the StepOnePlus RT-PCR system (Applied Biosystems) using the PerfeCTa SYBR Green FastMix (Quanta Biosciences). Relative gene expression was determined as $2^{\wedge -\Delta Ct}$, with ΔCt being the difference between the cycle threshold (Ct) value of the target gene and *Gapdh*. For semiquantitative expression analysis, PCR was performed and analyzed by gel electrophoresis. Amplification product intensities were determined using ImageJ software (NIH), and values were normalized and expressed as fold changes in gene expression over *GAPDH*. The following primers were used: h*ABCA1*-F, AACAGTTTGTGGCCCTTTTG; h*ABCA1*-R, AGTTCCAGGCTGGGGTACTT; h*LDL-R*-F, TCACTCCATCTCAAGCATCG; h*LDL-R*-R, GGTGGTCCTCTCACACCAGT; h*HMG-CoA-R*-F, GGCATTTGACAGCACTAGCA; h*HMG-CoA-R*-R, GCTGGAATGACAGCTTCACA; h*GAPDH*-F, GTCAGTGGTGGACCTGACCT; h*GAPDH*-R, Hs_*ABCA1*-SG QuantiTect Primer Assay (Qiagen); m*Abca1*-F, GGACATGCACAAGGTCCTGA; and m*Abca*1-R, CAGAAAATCCTGGAGCTTCAAA.

Mice treatment and analysis. BTBR (black and tan, brachiuric) *ob/ob* (leptin deficient) mice were purchased from The Jackson Laboratory. Mice were injected subcutaneously with 4,000 mg/kg CD or saline, as reported previously (39), three times per week for 5 months. Urine was collected and body weight and glycemia (OneTouch) were determined weekly. Six mice per group were analyzed. All animal procedures were approved by the Institutional Animal Care and Use Committee. After isotonic saline perfusion, the right kidney was removed for cholesterol content determination and mRNA extraction. One left kidney pole was embedded in optimal cutting temperature (OCT) and a second pole fixed in 4% paraformaldehyde and paraffin embedded for histological analysis. Blood samples were analyzed for complete blood count (CBC), lipid panel, aspartate aminotransferase (AST), alanine transaminase (ALT), alkaline phosphatase, γ-glutamyl transpeptidase (GGT), and blood urea nitrogen (BUN) in the Comparative Laboratory Core Facility (University of Miami). Serum creatinine was determined by tandem mass spectrometry at the UAB-UCSD O'Brien Core Center (University of Alabama at Birmingham) using the methods previously described (40). The urine albumin content was measured by ELISA (Bethyl Laboratories). Urinary creatinine was assessed by an assay based on the Jaffe method (Stanbio). Values are expressed as microgram albumin per milligram creatinine. Fasting plasma insulin was determined by ELISA (Mercodia, Uppsala, Sweden). Intraperitoneal glucose tolerance tests (IPGTTs) were performed 4 months after treatment; after 5 h fasting, blood glucose was recorded at baseline and up to 180 min after a glucose bolus (1.5 g/kg). For insulin sensitivity, glycemia was monitored at baseline and up to 150 min after intraperitoneal injection of 4 mU/g of short-acting insulin. Human islets from four different isolations were pretreated with 0.5 mmol/L CD for 1 h and perfused as described previously to determine insulin release in response to glucose and KCl (38).

Histology, assessment of mesangial expansion, and glomerular surface area. Periodic acid-Shiff (PAS) staining of 4-μm-thick tissue sections was performed. Twenty glomeruli per section were analyzed for mesangial expansion by semiquantitative analysis (scale 0–4) performed by two blinded independent

investigators. The glomerular surface was delineated in each encountered glomerulus and the mean surface area calculated as previously described (41).

Statistical analysis. Data are shown as mean and SD. Four to eight independent experiments were performed for in vitro studies. Six mice per group were used for in vivo experiments. Statistical analysis was performed with one-way ANOVA. When one-way ANOVA showed statistical significance, results were compared using Student *t* test after Tukey correction for multiple comparisons. Results were considered statistically significant at $P < 0.05$.

RESULTS

Clinical laboratory measurements and patient population. We studied 30 male subjects divided into three groups based on clinical characteristics at the time of collection of the sera samples. The study subjects included *1*) 10 patients with T1D, normoalbuminuria, and normal creatinine, defined as patients without DKD (DKD^-), *2*) 10 patients with T1D, albuminuria, and altered creatinine, defined as patients with DKD (DKD^+), and *3*) 10 healthy controls (C). The three groups were not significantly different for age, total cholesterol, HDL cholesterol, LDL cholesterol, and triglycerides. All diabetic patients were taking agents to block the renin-angiotensin-aldosterone system. Lipid-lowering agents were used in 2 of 10 controls, 3 of 10 DKD^-, and 4 of 10 DKD^+. Duration of diabetes, fasting plasma glucose, and HbA_{1c} were not significantly different among DKD^+ and DKD^- patients (Table 1). The mean estimated glomerular filtration rate (eGFR) was 101 mL/min/1.73 m^2 in DKD^-, 97 mL/min/1.73 m^2 in C, and 43 mL/min/1.73 m^2 in the DKD^+ group. Sera collected 6 ± 1.2 years prior from five of the patients with DKD (mean eGFR declined from 109 to 75 mL/min/1.73 m^2) were used in selected experiments.

Podocytes exposed to DKD^+ sera have a characteristic cRNA signature. RNA was extracted from differentiated podocytes cultured in the presence of patient sera as we previously reported (14). Gene heatmap analysis (Agilent Technologies) revealed strong regulation of several GSEA KEGG pathways with dysregulation of genes involved in actin cytoskeleton regulation, insulin signaling, cytokines and cytokine receptor interaction primarily through TLR4, tumor necrosis factor-α, and interleukin-1β, and apoptosis (Fig. 1*A*). Microarray data are available at http://www.ncbi.nlm.nih.gov/geo/query/acc.cgi?acc=GSE46900. We validated these findings at the protein level, demonstrating by Western blotting that in DKD^+-treated podocytes, MyD88 expression was increased (Fig. 1*B*), the ability of insulin to phosphorylate AKT was impaired (Fig. 1*C*), and the amount of cleaved caspase 3 was increased (Fig. 1*D*).

TABLE 1
Clinical characteristics of the patients with T1D (with or without DKD) and their respective controls

	C (n = 10)	DKD^- (n = 10)	DKD^+ (n = 10)
Age	44 ± 11	48 ± 7	49 ± 9
Sex	M/F (10/0)	M/F (10/0)	M/F (10/0)
Diabetes duration	—	29 ± 11	32 ± 10
HbA_{1c} (%)	5.5 ± 0.3	7.9 ± 0.8	7.9 ± 1.2
(mmol/mol)	37 ± 3.3	63 ± 8.8	63 ± 13
FPG (mg/dL)	81 ± 19	102 ± 12	92 ± 26
Serum creatinine (mg/dL)	0.9 ± 0.1	0.8 ± 0.1	1.7 ± 0.9**
Total cholesterol (mg/dL)	182 ± 23	170 ± 23	166 ± 54
HDL cholesterol (mg/dL)	56 ± 12	74 ± 14	64 ± 16
LDL cholesterol (mg/dL)	105 ± 24	79 ± 14	82 ± 48
Triglyceride (mg/dL)	96 ± 37	67 ± 23	103 ± 44

Data are mean ± SD. FPG, fasting plasma glucose. F, female; M, male. **$P < 0.01$, when comparing DKD^+ to DKD^- and C.

Normal human podocytes exposed to sera of patients with DKD exhibit cell blebbing. Podocytes exposed to the sera of patients with DKD experienced pronounced actin cytoskeleton remodeling with localized decoupling of the cytoskeleton from the plasma membrane (blebbing), which was evident in both the phalloidin staining (F-actin) and the bright field images (Fig. 2*A*) and which was very different from what we have reported in focal and segmental glomerulosclerosis (14). Quantitative analysis of cell blebbing (percentage of cells with blebs out of a total of 200 consecutive cells analyzed) revealed this phenotype in 80% of cells exposed to DKD^+ sera, but in only 20% of cells exposed to DKD^- sera and 5% in the controls ($P < 0.001$) (Fig. 2*B*). Cell blebbing was accompanied by the redistribution of active RhoA at the site of cell blebbing (Fig. 2*C*) and by an increase in total RhoA (Fig. 2*D*). Cell blebbing was not a consequence of reduced GFR in the DKD^+ group, as historical sera collected from five of the patients with T1D and normal GFR that ultimately developed DKD caused the same degree of cell blebbing in cultured podocytes as the sera from the same patients collected on average 6 ± 1.2 years later, when the patients had established DKD with macroalbuminuria and low GFR (Fig. 2*E*).

Impaired reverse cholesterol transport in podocytes exposed to DKD^+ sera and in glomeruli from patients with early diabetes. As inflammation, insulin resistance, apoptosis, and cytoskeleton remodeling are linked by the intracellular accumulation of lipids in the pathogenesis of nonalcoholic steatohepatitis (NASH syndrome) (42), and accumulation of cholesterol has been described in the cortex of the kidneys of mice with DKD (20), we explored if podocytes cultured in the presence of sera of patients with DKD accumulate intracellular cholesterol. We were able to demonstrate an increased number of ORO- (Fig. 3*A* and *C*) and filipin-positive cells (Fig. 3*B*) in DKD^-- and DKD^+-treated cells, more so in the DKD^+-treated cells. Quantitative analysis of total (Fig. 3*D*), free (Fig. 3*E*), and esterified cholesterol (Fig. 3*F*) revealed significantly increased esterified cholesterol in DKD^+-treated cells when compared with cells treated with sera from control subjects. This increase was likely due to impaired cholesterol efflux, as LDL receptor and HMG-CoA reductase expression were unchanged (Fig. 3*G* and *H*) whereas *ABCA1* mRNA expression was downregulated in DKD^+-treated podocytes (Fig. 3*I*). We then studied the mRNA expression of lipid-related genes in glomeruli from an additional 70 patients with T2D and early DKD when compared with 32 normal living donors (Supplementary Table 1) and demonstrated significant downregulation of *ABCA1* in DKD (Fig. 3*J*). Interestingly, downregulation of *ABCA1* mRNA expression was a feature of DKD only, as *ABCA1* was not regulated in other proteinuric glomerular diseases (Fig. 3*J*), such as membranous nephropathy (n = 21) and focal segmental glomerulosclerosis (FSGS, n = 18). In order to assess if downregulation of *ABCA1* expression is associated with physiologically decreased cholesterol efflux in DKD sera–treated human podocytes, we performed cholesterol efflux assays using [^{3}H]cholesterol. When cholesterol-labeled podocytes were incubated with 0.5% serum from patients for 6 h, both DKD^- ($P < 0.01$) and DKD^+ ($P < 0.001$) serum were significantly less effective at promoting cholesterol efflux compared with C serum (Fig. 3*K*). These results indicate that downregulation of *ABCA1*

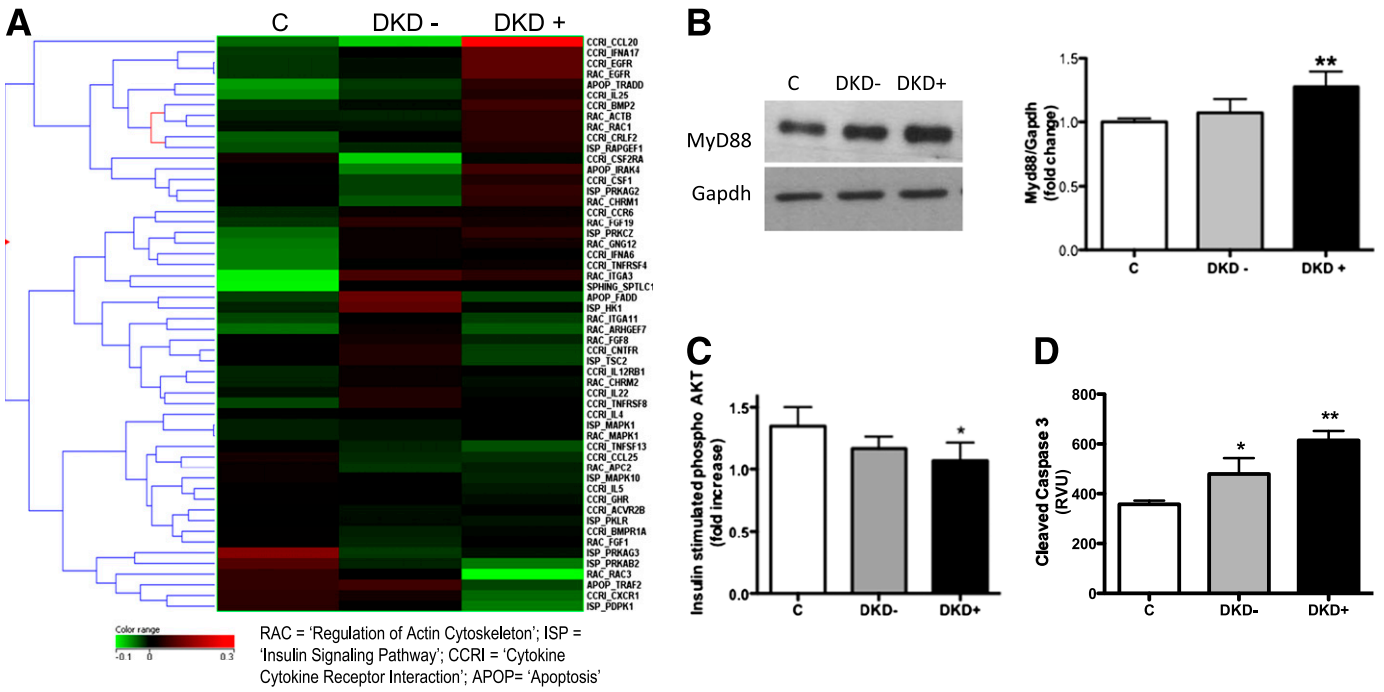

FIG. 1. Expression analysis of podocytes cultured with patient sera. *A*: cRNA beadchip analysis was performed using cRNA isolated from human podocytes exposed to pooled sera from control patients and patients without (DKD$^-$) or with kidney disease (DKD$^+$). Quadruplicate expression data analysis was performed after batch correction. Significant probes (n = 1,015) were identified as differentially expressed between DKD$^-$ and DKD$^+$, and pathway analysis revealed that four major pathways were modulated as shown in the heatmap. *B*: Bar graph analysis (mean ± SD) and representative Western blot analysis of four independent experiments demonstrating increased MyD88 protein expression in DKD$^+$-treated podocytes when compared with C. **$P < 0.01$. *C*: Bar graph analysis (mean ± SD) of fold changes in phosphorylated AKT/total AKT after insulin stimulation in four different experiments. Data were analyzed with Luminex technology and demonstrated decreased cellular insulin sensitivity in DKD$^+$- and DKD$^-$-treated cells when compared with C. *$P < 0.05$. *D*: Bar graph analysis (mean ± SD) of cleaved caspase 3 analyzed in four independent experiments, demonstrating increased cleaved caspase 3 in DKD$^+$-treated cells when compared with C. *$P < 0.05$; **$P < 0.01$. RVU, relative value units.

expression in DKD$^+$ sera–treated podocytes is associated with impaired cholesterol efflux, which may partially account for the cellular cholesterol observed differences.

CD protects podocytes in vitro. As the exposure of podocytes in culture to DKD$^+$ sera caused accumulation of total cholesterol in association with decreased *ABCA1* expression, a transporter responsible for cholesterol efflux, we went on to test the hypothesis that CD would protect podocytes from the actin cytoskeleton remodeling and cell blebbing observed after exposure to the sera from patients with DKD. We were able to demonstrate that CD prevented cell blebbing and the localization of phosphorylated caveolin to focal adhesion sites (Fig. 4*A*). Quantitative cholesterol analysis showed that CD prevented the accumulation of total and esterified cholesterol in DKD$^+$-treated podocytes (Fig. 4*B* and *C*). Furthermore, prevention of intracellular cholesterol accumulation with CD also prevented DKD$^+$-induced apoptosis (Fig. 4*D*), insulin resistance (Fig. 4*E*), and MyD88 expression (Fig. 4*F*). Blockade of HMG-CoA reductase with simvastatin in podocytes did not protect from DKD$^+$-induced actin cytoskeleton remodeling (Supplementary Fig. 1).

Subcutaneous administration of CD protects BTBR *ob/ob* mice from the development of DKD. BTBR *ob/ob* mice have been described as a mouse model of progressive DKD (43). After establishing a dose and a mode of administration based on preliminary toxicology studies, we treated 4-week-old BTBR mice with subcutaneous administration of three weekly injections of 2-hydroxypropyl-β-cyclodextrin (4,000 mg/kg body weight) for 5 months. Although no changes in AERs were observed up to 2 months after treatment initiation in homozygous mice, at 3 months, a significant downregulation of the albumin/creatinine ratios was observed in the morning spot urine samples ($P < 0.001$) in CD-treated when compared with untreated BTBR *ob/ob* mice. This decrease persisted until sacrifice (5 months after initiation of treatment) (Fig. 5*A*). At sacrifice, CD-treated mice showed a reduction of kidney weight (Fig. 5*B*). CD did not affect *ABCA1* mRNA expression in the kidney cortex (Fig. 5*C*) but resulted in a significant reduction of total cholesterol (Fig. 5*D*). BUN and creatinine were not significantly affected by CD treatment (Fig. 5*E* and *F*). However, CD treatment resulted in a reduction of mesangial expansion (Fig. 5*G* and *H*) without affecting the glomerular surface area (Fig. 5*I*). After 4 months of treatment, we also observed a reduction of body weight (Fig. 6*A* and *B*), which was accompanied by a concomitant improvement of random glycemia (Fig. 6*C*). Furthermore, sera collected at sacrifice demonstrated a significant improvement of fasting plasma insulin and fasting plasma glucose (Fig. 6*D* and *E*). IPGTTs performed 1 week prior to sacrifice were improved in CD-treated homozygous mice when compared with homozygous controls (Fig. 6*F*). As improvement was observed despite a similar insulin sensitivity test (Fig. 6*G*), we analyzed the effect of low-dose CD on the function of four different preparations of human islet cells. A significant improvement in glucose-stimulated insulin release was observed in CD-treated human islets when compared with untreated human islets (Fig. 6*H*). To determine whether the beneficial

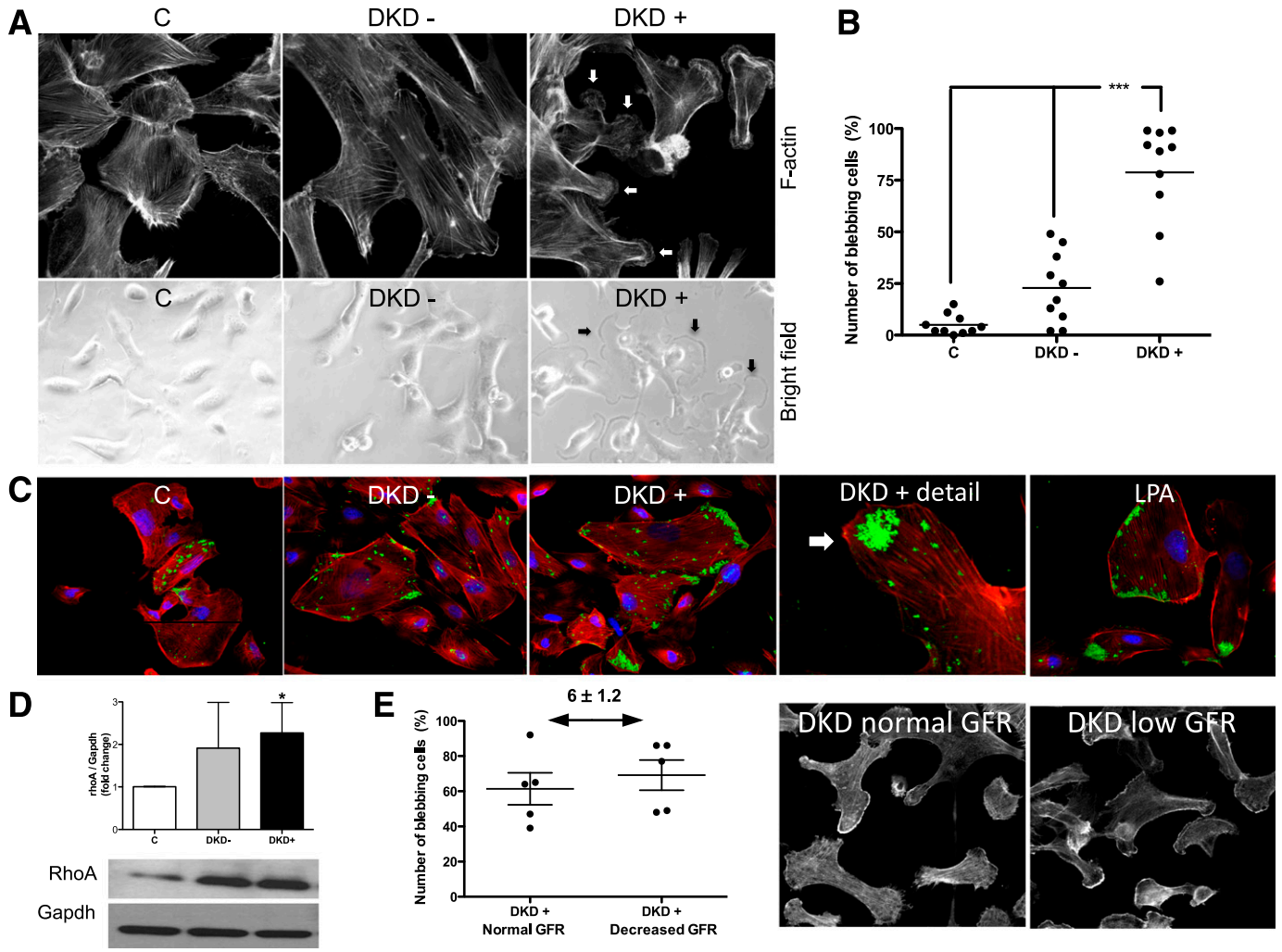

FIG. 2. Actin remodeling in DKD$^+$ sera–treated podocytes. ***A*: Representative F-actin staining (*top*) and bright field images (*bottom*) of podocytes exposed to DKD$^+$ sera when compared with C and DKD$^-$ sera, demonstrating cell blebbing in DKD$^+$ serum–treated cells. White and black arrows point to areas of cell blebbing. *B*: Quantitative analysis of cell blebs (mean ± SD) observed in podocytes exposed to individual DKD$^+$ sera when compared with DKD$^-$ and C. ***$P < 0.001$. *C*: Representative immunofluorescence images demonstrating the localization of active RhoA (green) at the sites of cell blebbing in DKD$^+$ serum–treated podocytes. Lysophosphatidic acid (LPA)–induced RhoA activation was used as positive control. F-actin is visualized in red (rhodamine phalloidin) and nuclei in blue (DAPI). *D*: Bar graph analysis (mean ± SD) and representative Western blot of four independent experiments demonstrating increased total RhoA in DKD$^+$ serum–treated podocytes when compared with C. *$P < 0.01$. *E*: Quantitative analysis (mean ± SD) of the number of podocytes showing cell blebbing after exposure to the sera of five patients with DKD$^+$ and decreased GFR when compared with the sera collected from the same five patients 6 years prior when they had normal GFR. No significant differences were observed. A representative F-actin staining of cell blebbing is also shown. Clinical characteristics of the patients are shown in Supplementary Table 2.**

effect of CD on islet cell function was associated with the modulation of ABCA1 expression in pancreatic islets, we performed immunofluorescence staining using a rabbit polyclonal ABCA1 antibody (gift from A.M.) and determined ABCA1 expression as mean fluorescence intensity per pancreata analyzed (Fig. 6*I*). As expected, pancreata from homozygous BTBR *ob/ob* mice were characterized by significantly decreased ABCA1 expression when compared with heterozygous littermates ($P < 0.001$), and CD treatment significantly increased ABCA1 expression in the pancreata of homozygous BTBR *ob/ob* ($P < 0.001$) and heterozygous BTBR *ob*/+ mice ($P < 0.01$). As hemolytic anemia and liver toxicity have been described while using other CD derivatives in rodents and humans (26), and because we administered high-dose CD for a period of 5 months, we studied hemoglobin, AST, ALT, and GGT at sacrifice. No abnormalities due to chronic CD administration were observed, indicating that the chronic use of CD is not accompanied by adverse side effects. Total cholesterol was increased in CD-treated mice after 3 months of treatment (Table 2).

DISCUSSION

As diabetes is a multifactorial disorder, it has been difficult to prevent or cure diabetes complications by targeting specific risk factors such as hyperglycemia and hypertension. In fact, even in the setting of multifactorial intervention, a subset of patients still develop DKD in both T1D and T2D (2,3). Evidence points to a strong cross-talk between different target organs in diabetes (44), which raises the possibility that multiple circulating factors other than glucose may directly affect podocyte function in DKD. In order to identify the key pathways that are activated in podocytes irrespectively of the nature of circulating factors, we used a cell-based bioassay where human podocytes

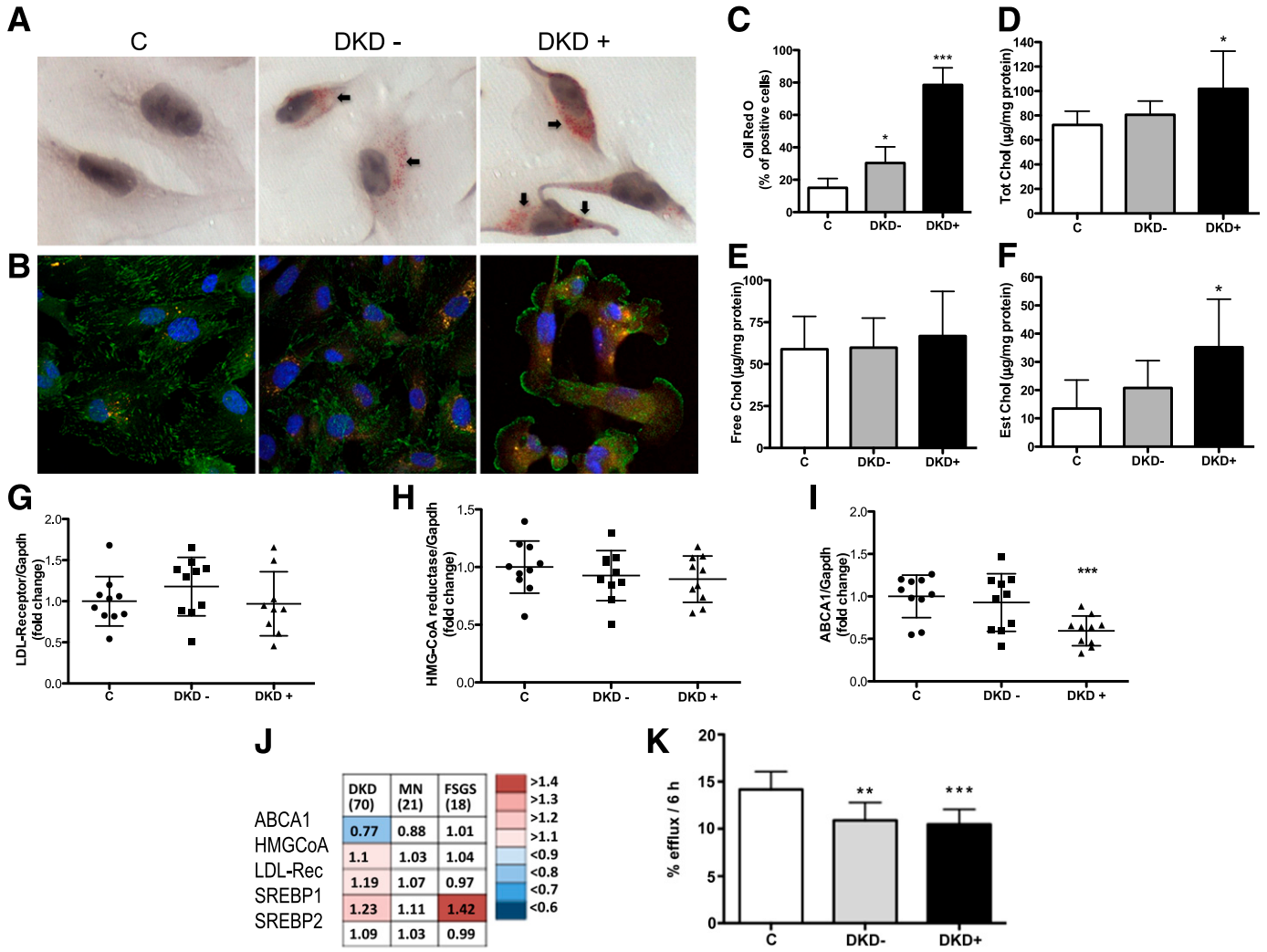

FIG. 3. Cholesterol accumulation in podocytes exposed to DKD$^+$ sera. *A*: Representative ORO staining of podocytes exposed to DKD$^+$ sera when compared with C and DKD$^-$ sera. Black arrows point to spots of major lipid droplet accumulation. *B*: Representative filipin staining (orange) and phosphorylated caveolin staining (green) of podocytes exposed to DKD$^+$ sera when compared with C and DKD$^-$. *C*: Bar graph quantitative analysis (mean ± SD) of ORO-positive cells in podocytes exposed to the pools of sera from 10 patients with DKD$^-$ or DKD$^+$ or to pools of the sera from controls, demonstrating that exposure to both DKD$^-$ and DKD$^+$ sera causes significant lipid droplet accumulation in cultured human podocytes. *P < 0.05; ***P < 0.001. *D–F*: Bar graph analysis (mean ± SD) of total cholesterol (Tot C), free cholesterol (Free C), and esterified cholesterol (Est C) as determined via enzymatic reaction in podocytes exposed to pools of DKD$^+$ sera when compared with C and DKD$^-$. *P < 0.05. *G–I*: Quantitative RT-PCR analysis (mean ± SD) of LDL receptor HMG-CoA reductase and ABCA1 expression in podocytes exposed to individual patient sera. ***P < 0.001. *J*: Expression analysis of glomerular gene expression of lipid-related genes in 70 patients with early DKD, 21 patients with membranous nephropathy (MN), and 18 patients with FSGS when compared with 32 living donors. Numbers reflect fold change in disease when compared with living donors. Genes passing an FDR correction (qvalue) for multiple testing <5% were considered significantly regulated genes with significant changes in gene expression and are highlighted by blue or red background colors. *K*: Cholesterol efflux assay demonstrating decreased cholesterol efflux after 6 h in podocytes treated with DKD$^-$ (P < 0.01) and DKD$^+$ (P < 0.001) sera when compared with C. **P < 0.01; ***P < 0.001.

exposed to sera of healthy individuals were compared with human podocytes exposed to sera of patients with long-lasting diabetes without DKD (DKD$^-$) and to sera of patients with long-lasting diabetes and nephropathy (DKD$^+$). We have successfully used this bioassay to identify predictors for the development of proteinuria in another glomerular disorder caused by circulating permeability factors, i.e., focal and segmental glomerulosclerosis (14).

Our results demonstrate that DKD$^+$ sera–treated podocytes have a characteristic microarray signature, which allows distinguishing them from DKD$^-$ or control serum–treated podocytes. In addition, we identified four key pathways differentially regulated in DKD$^+$ when compared with DKD$^-$: inflammation, insulin resistance, apoptosis, and actin cytoskeleton remodeling (Figs. 1 and 2). Differently from what we described for FSGS, rearrangements of the actin cytoskeleton observed in DKD$^+$ sera–treated podocytes were typical of cell blebbing, as the cell protrusions were vimentin negative (data not shown) (45) but were accompanied by increased RhoA activity (46). These characteristics have been described to differentiate cell blebs from lamellipodia and may be the consequence of the concomitant activation of caspase 3 (47,48). A modulation of these four major pathways has been described in the pathogenesis of NASH and it has been related to the accumulation of intracellular cholesterol (42), a known modulator of actin cytoskeleton remodeling (49). Interestingly, cholesterol accumulation was also described in the kidney from experimental models of diabetes that resemble T1D and T2D (19,20), in a similar fashion to what

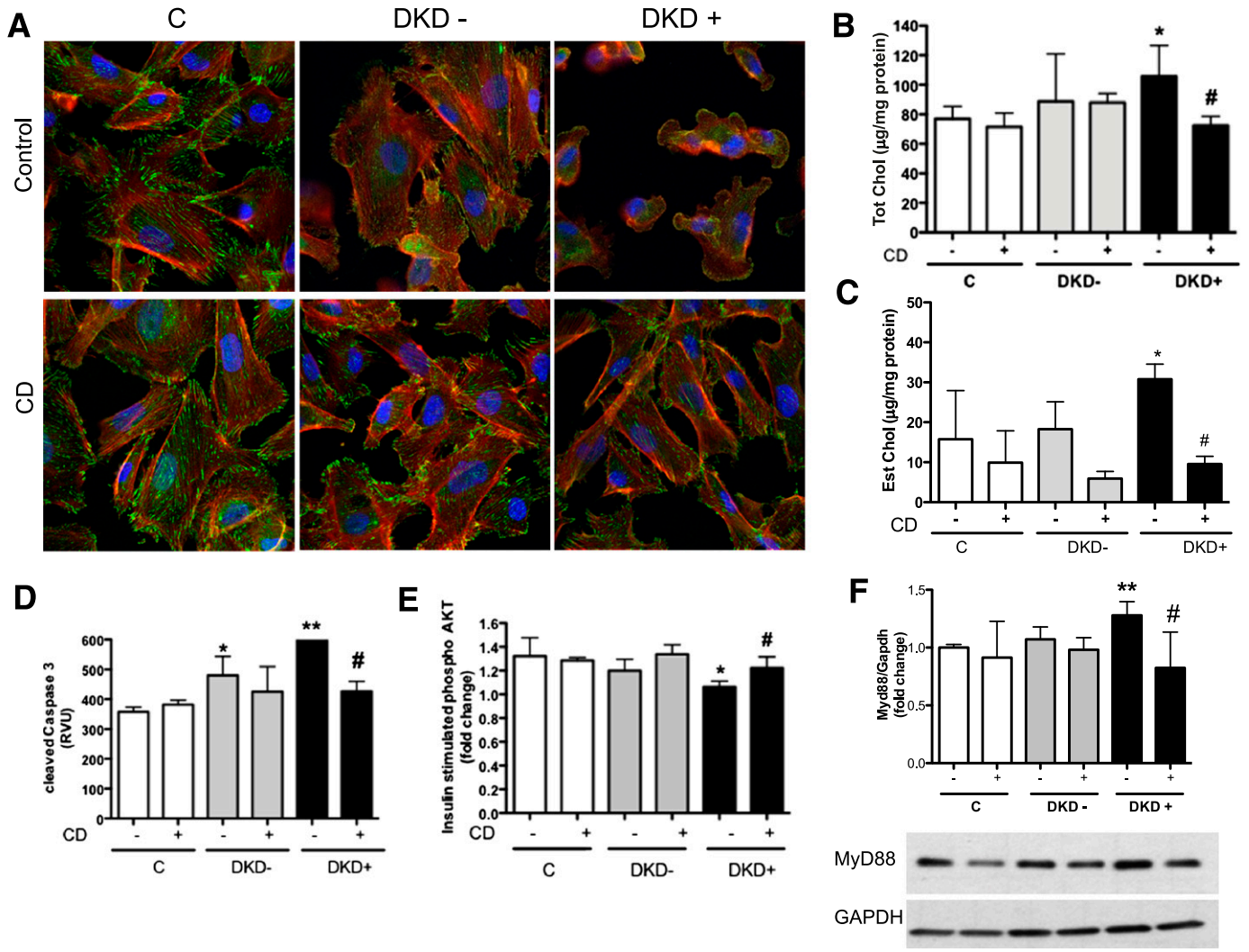

FIG. 4. CD protects podocytes from changes observed after exposure to DKD⁺ sera. *A*: Representative phalloidin (red) and phosphorylated caveolin (green) confocal images of normal human podocytes exposed to DKD⁺ sera when compared with C and DKD⁻ sera in the presence (CD) or absence (control) of CD. DAPI (blue) was used to identify nuclei. Bar graph analysis (mean ± SD) of the effect of CD on total (*B*) and esterified cholesterol (*C*) in CD-treated (+) vs. untreated (−) podocytes exposed to DKD⁺ sera when compared with C and DKD⁻ sera. **P* < 0.05, when comparing DKD⁺ vs. C. #*P* < 0.05, when comparing CD-treated vs. untreated podocytes in the same group. *D–F*: Bar graph analysis (mean ± SD) of cleaved caspase 3, insulin-stimulated AKT phosphorylation, and MyD88 expression in CD-treated (+) vs. untreated (−) podocytes exposed to DKD⁺ sera when compared with C and DKD⁻ sera. **P* < 0.05 and ***P* < 0.01, when comparing DKD⁺ vs. C. #*P* < 0.05, when comparing CD-treated vs. untreated podocytes in the same group. RVU, relative value units.

was initially reported for glycosphingolipids in rodents with DKD (50). We therefore studied the intracellular cholesterol content in podocytes exposed to the sera of patients with DKD, and we found an increase of both total and esterified cholesterol (Fig. 3). This finding is different from the accumulation of lysosomal free cholesterol as observed when Niemann-Pick C proteins 1 and 2 are mutated (51). Interestingly, the accumulation of cholesterol in podocytes treated with DKD⁺ sera was likely the consequence of reverse cholesterol transport, as a strong downregulation of *ABCA1* mRNA was observed. In addition, experiments using [^{3}H]cholesterol showed impaired cholesterol efflux in human podocytes treated with 0.5% DKD⁻ and DKD⁺ sera for 6 h (Fig. 4), which may partially account for the differences we observed in the cellular cholesterol content in DKD⁺ sera–treated human podocytes. Downregulation of *ABCA1* was furthermore confirmed in mRNA transcripts isolated from the glomeruli of 70 patients with T2D and early DKD. In diabetes, accumulation of cholesterol in peripheral tissue targets of diabetes complications has been described and linked to insulin resistance (52). Increased fat fraction has also been described in the pancreas of obese adolescent and diabetic patients (53) and has been shown to impair pancreatic β-cell function and insulin granule exocytosis (54).

How cholesterol accumulation occurs, irrespective of hypercholesterolemia, has been studied in humans and experimental animals. In the NOD mouse model of T1D, *ABCA1* proteins are downregulated in both kidneys and circulating macrophages (18). In humans, *ABCA1* genetic variants are strongly associated with the risk of coronary artery disease (16) and cholesterol efflux capacity of macrophages inversely correlates with carotid and coronary artery lesions (36). Elegant studies using the sera of patients with and without diabetic nephropathy in a cell-based assay to determine cholesterol efflux capacity in macrophages have demonstrated that the capacity of the sera to induce *ABCA1*-mediated cholesterol efflux was impaired

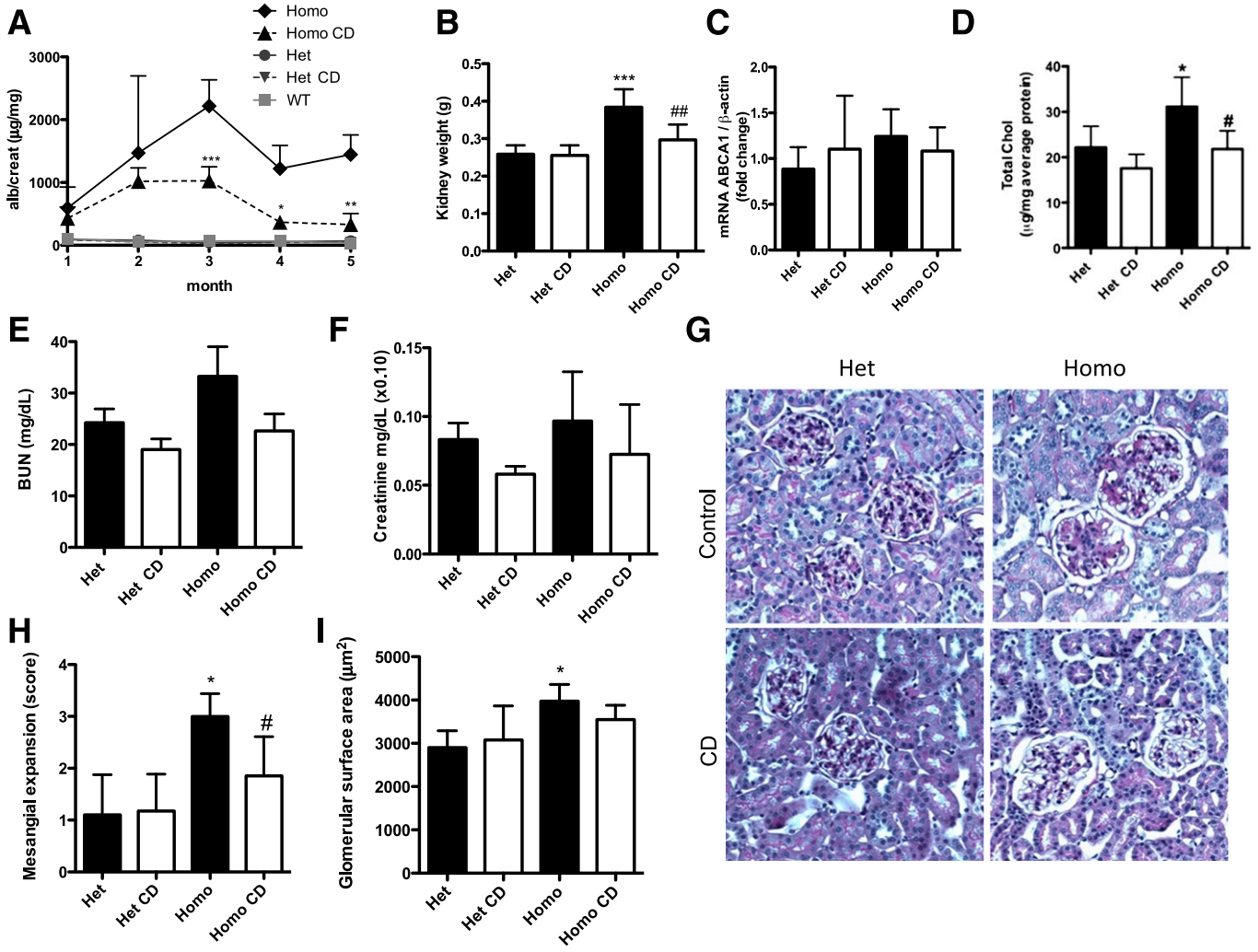

FIG. 5. CD protects from DKD in vivo. *A*: CD administered to homozygous and heterozygous BTBR *ob/ob* mice subcutaneously three times a week (n = 6 per group) resulted in a reduction in albumin/creatinine ratios (mean ± SD) starting at 3 months after the initiation of the treatment. *P < 0.05; **P < 0.01; ***P < 0.001. *B*: Kidney weight (mean ± SD) was significantly increased in homozygous mice (*P < 0.001), and such an increase was prevented by CD treatment (##P < 0.01). *C*: Bar graph analysis (mean ± SD) of the effect of CD on *ABCA1* mRNA expression in kidney cortexes of homozygous and heterozygous BTBR *ob/ob* mice. *D*: Bar graph analysis (mean ± SD) of the effect of CD on the total cholesterol content in kidney cortexes of homozygous and heterozygous BTBR *ob/ob* mice. *E* and *F*: Bar graph analysis (mean ± SD) showing that serum BUN and creatinine concentrations remain unchanged after CD treatment of the mice. Measurements were performed on serum obtained from the mice at sacrifice. *G*: Representative PAS staining of kidney sections from homozygous and heterozygous BTBR *ob/ob* mice after 5 months of treatment with either CD or vehicle. Bar graph analysis (mean ± SD) of the scores for mesangial expansion (*H*) and of the glomerular surface area (*I*) on PAS-stained kidney sections from homozygous and heterozygous BTBR *ob/ob* mice after 5 months of treatment with either CD or vehicle were assessed by two blinded, independent investigators. *P < 0.05, when comparing DKD$^+$ vs. C. #P < 0.05, when comparing CD-treated vs. untreated mice in the same group. Het, heterozygous; Homo, homozygous; WT, wild type.**

in patients with T2D and incipient or overt nephropathy (17). As systemic downregulation of *ABCA1* also results in impaired pancreatic β-cell function (54), strategies that maintain cellular cholesterol homeostasis may be beneficial for the treatment of diabetes and its related complications. Supporting these observations and our results presented here, a recent study showed that inhibition of miR-33a, which leads to increased ABCA1 expression, is sufficient to normalize insulin secretion and cellular cholesterol levels in pancreatic islets (55).

In order to demonstrate that increased intracellular cholesterol is necessary for DKD$^+$ sera to cause actin remodeling and apoptosis, we used pharmacological interventions targeting cellular cholesterol homeostasis prior to exposure to sera from patients. Statins were used to decrease intracellular cholesterol synthesis in podocytes, and CD was used to remove cholesterol from cultured podocytes prior to exposure to patient sera. Although statins did not protect podocytes in our model (Supplementary Fig. 1), CD significantly protected podocytes from apoptosis, insulin resistance, inflammation, and cell blebbing (Fig. 4), an observation that is consistent with the fact that cells exposed to DKD$^+$ sera showed cholesterol accumulation due to an impairment of reverse cholesterol transport rather than increase in intracellular cholesterol synthesis. As strategies that raise HDL cholesterol have been proven ineffective in reducing events (56) and HDL levels may not correlate to cholesterol efflux (36), we used CD as a potent cholesterol acceptor. We administered CD in vivo to BTBR *ob/ob* mice to test if this would result in preservation of kidney function and reduction of albuminuria. We found that CD administered in vivo for 5 months partially

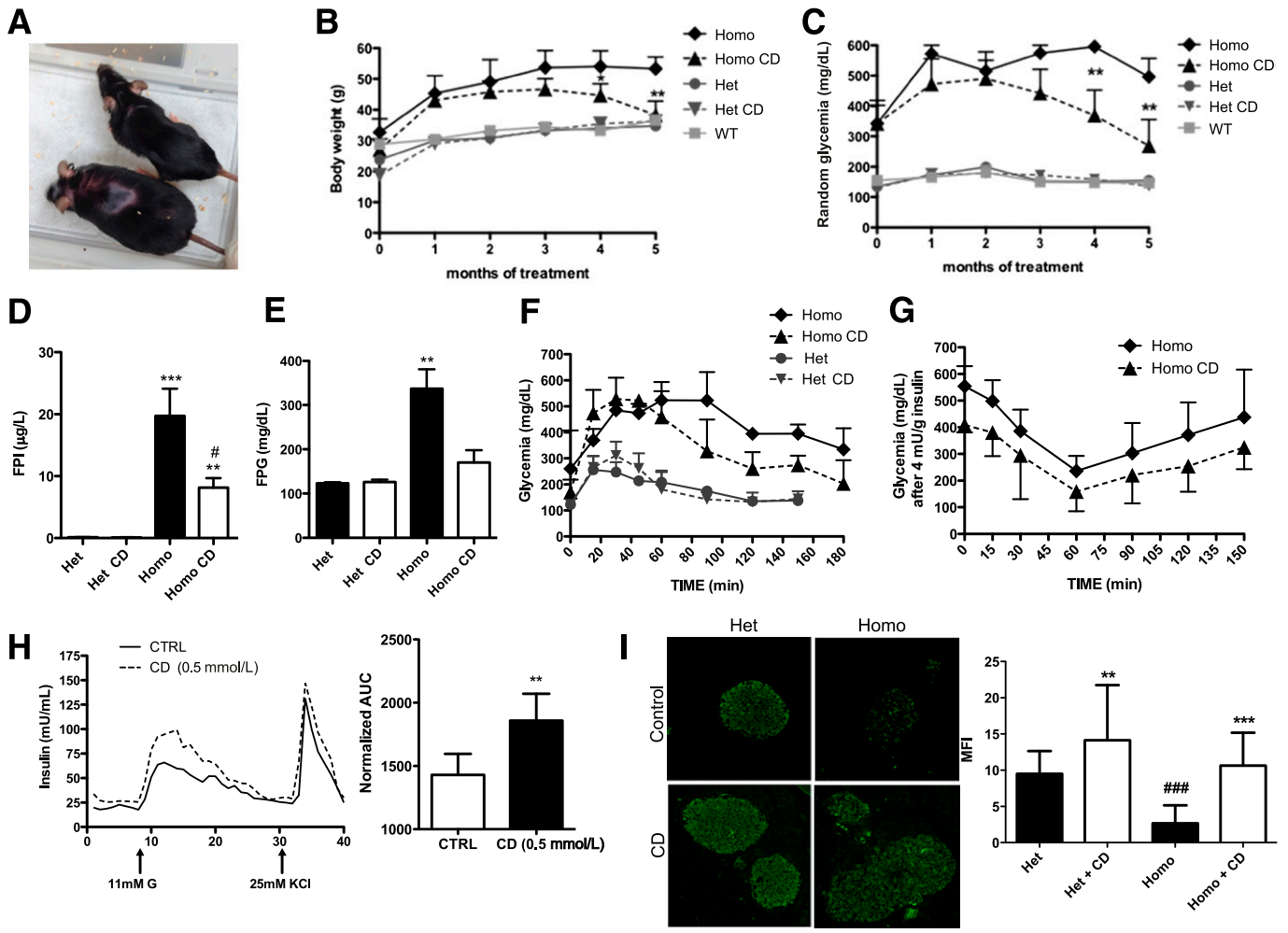

FIG. 6. CD improves diabetes in vivo. *A* and *B*: CD administered to homozygous and heterozygous BTBR *ob/ob* mice subcutaneously three times a week ($n = 6$ per group) resulted in a significant reduction in body weight (mean ± SD) starting at 4 months after the initiation of the treatment. *$P < 0.05$; **$P < 0.01$. *C*: CD administered to homozygous BTBR *ob/ob* mice resulted in a significant reduction in random glycemia (mean ± SD) starting at 4 months after the initiation of the treatment. Bar graph analysis (mean ± SD) of fasting plasma insulin (FPI) and glucose concentrations. FPI ($P < 0.01$; ***$P < 0.001$; #$P < 0.05$) (*D*) and fasting plasma glucose (FPG) (**$P < 0.01$) (*E*) were significantly increased in homozygous mice when compared with heterozygous controls. The increase was prevented by CD treatment (#$P < 0.05$). *F*: IPGTTs performed at 5 months after the initiation of the CD treatment showed improved glucose tolerance in CD-treated BTBR *ob/ob* mice when compared with untreated BTBR *ob/ob* mice. *G*: CD treatment did not affect the sensitivity to a single dose of short-acting insulin (4 mU/g) in BTBR *ob/ob* mice. *H*: Representative perifusion experiment and bar graph analysis of the area under the curve demonstrating the effect of 0.5 mmol/L CD on glucose-stimulated insulin release in human pancreatic islets from four independent donors (**$P < 0.01$). *I*: Immunofluorescence staining for ABCA1 reveals increased ABCA1 expression in pancreata of CD-treated BTBR *ob/ob* mice when compared with untreated littermates (*left*). Bar graph analysis (*right*) showing that pancreata isolated from homozygous BTBR *ob/ob* mice are characterized by significantly decreased ABCA1 expression when compared with heterozygous littermates (###$P < 0.001$). CD treatment significantly increased ABCA1 expression in pancreata of homozygous BTBR *ob/ob* (***$P < 0.001$) and heterozygous BTBR *ob*/+ mice (**$P < 0.01$). AUC, area under the curve; CTRL, control; Het, heterozygous; Homo, homozygous; MFI, mean fluorescent intensity; WT, wild type.**

reduced albuminuria and prevented mesangial expansion (Fig. 5). Impairment of liver function and hemolytic anemia were not observed. CD treatment effectively reduced the total kidney cholesterol content but did not affect *ABCA1* mRNA expression in kidney cortexes. As CD was administered systemically and cells other than kidney cells are characterized by accumulation of intracellular cholesterol, we investigated if CD had any effect on the metabolic profile of BTBR *ob/ob* mice. Indeed, CD-treated diabetic mice experienced a significant reduction of their body weight and of their glycemia after 4 months of treatment, which was associated with an upregulation of ABCA1 expression in pancreatic islets and with the improvement of glucose-stimulated insulin release in human islets in vitro (Fig. 6). Further studies are needed to identify the factor(s) primarily responsible for intracellular cholesterol accumulation in diabetes and the exact mechanisms of CD protection in diabetes and DKD.

In conclusion, using an assay in which normal human podocytes are cultured with the sera of patients with DKD, we have shown that circulating factors other than glucose may directly affect podocyte function in vitro. We uncovered a novel mechanism in which intracellular cholesterol accumulation due to impaired efflux plays a central role in podocyte injury in vitro. These data suggest that this mechanism may contribute to the development and/or the progression of DKD. Furthermore, using CD in our in vitro and in vivo studies, we were able to protect podocytes from injury caused by intracellular cholesterol accumulation, indicating that CD may represent a safe, FDA approved, effective way to target reverse cholesterol

TABLE 2
Serology of BTBR heterozygous and homozygous mice treated with CD

	Het	Het+CD	Homo	Homo+CD
Hb (g/dL)	15.9 ± 0.9	16.5 ± 0.6	14.5 ± 3.7	15.1 ± 1.2
AST (units/L)	146 ± 25	111 ± 44	143 ± 78	157 ± 26
ALT (units/L)	12 ± 7	14 ± 9	22 ± 13	37 ± 22
GGT (units/L)	5.2 ± 2.5	4.6 ± 0.3	6.5 ± 3.5	5.2 ± 2.3
Cholesterol (mg/dL)	46 ± 7	105 ± 9###	95 ± 4***	197 ± 17###

Data are mean ± SD. CD, 2-hydroxypropyl-β-cyclodextrin; Hb, hemoglobin; Het, heterozygous; Homo, homozygous. ***$P < 0.001$, when comparing Homo to Het. ###$P < 0.001$, when comparing CD treated vs. controls.

transport in diabetes and DKD. These observations underline the need to design safety and efficacy clinical trials to study the use of 2-hydroxypropyl-β-cyclodextrin in DKD.

ACKNOWLEDGMENTS

A.F. is supported by the NIH (DK-090316), the Forest County Potawatomi Community Foundation, the Max and Yetta Karasik Family Foundation, the Diabetes Research Institute Foundation, the Nephcure Foundation, and the Peggy and Harold Katz Family Foundation. The project described was supported by Grant 1UL1-TR-000460, (University of Miami Clinical and Translational Science Institute), the National Center for Advancing Translational Sciences, and the National Institute on Minority Health and Health Disparities. The authors acknowledge support from the University of Michigan and UAB-UCSD O'Brien Core Center (NIH 1P30-DK-081943 and -079337) for this project. This study was also supported by the Intramural Research Program of the National Institute of Diabetes and Digestive and Kidney Diseases, the Folkhälsan Research Foundation (P.-H.G.), the Wilhelm and Else Stockmann Foundation (P.-H.G., M.I.L., M.L., and C.F.), the Waldemar von Frenckell Foundation (M.I.L.), and the Liv och Hälsa Foundation (M.I.L. and P.-H.G.). Gene expression data from nondiabetic glomerular disease were provided by the European Renal cDNA Bank–Kroener-Fresenius Biopsy Bank supported by the Else-Kroener Fresenius Foundation members (Supplementary Data 2). This research was conducted using the resources of the University of Miami Center for Computational Science.

A.F., S.M.-G., and G.W.B. are inventors on issued and pending patents related to the diagnosis and treatment of proteinuric renal diseases and stand to gain royalties from their future commercialization. No other potential conflicts of interest relevant to this article were reported.

The funders had no role in study design, data collection and analysis, decision to publish, or preparation of the manuscript.

S.M.-G. conceived the project, designed and supervised the study, performed the in vitro and in vivo experiments, analyzed the data, and wrote the manuscript. J.G., R.A.-P., T.Y., R.V., and D.M. performed the in vitro and in vivo experiments. C.E.P. performed the in vitro and in vivo experiments and designed and performed experiments related to cholesterol determination and cholesterol efflux. M.L., M.I.L., C.F., and P.-H.G. performed some of the experiments and collected patient samples and clinical information. A.M. and R.G. designed and performed experiments related to cholesterol determination and cholesterol efflux. K.J. processed all the histology. V.N., A.R., M.K., and R.G.N. collected DKD microarray data and the patient clinical data. G.W.B. conceived one of the techniques utilized. A.F. conceived the project, designed and supervised the study, analyzed the data, and wrote the manuscript. A.F. is the guarantor of this work and, as such, had full access to all the data in the study and takes responsibility for the integrity of the data and the accuracy of the data analysis.

Part of this research was presented at the 71st Scientific Sessions of the American Diabetes Association, San Diego, California, 24–28 June 2011.

The authors acknowledge laboratory technicians and nurses M. Parkkonen, A. Sandelin, and J. Tuomikangas (Folkhälsan Institute of Genetics) for their skillful technical assistance. The authors also acknowledge the physicians and nurses at each study center (Supplementary Data 3). The authors thank Dr. Biju Isaac (Bioinformatics Core, University of Miami) for his assistance in submitting GEO data.

REFERENCES

1. U.S. Renal Data System. *USRDS 2011 Annual Data Report: Atlas of Chronic Kidney Disease and End-Stage Renal Disease in the United States*. Bethesda, MD, National Institutes of Health, National Institute of Diabetes and Digestive and Kidney Diseases, 2011
2. Gaede P, Lund-Andersen H, Parving HH, Pedersen O. Effect of a multifactorial intervention on mortality in type 2 diabetes. N Engl J Med 2008; 358:580–591
3. Hovind P, Tarnow L, Rossing K, et al. Decreasing incidence of severe diabetic microangiopathy in type 1 diabetes. Diabetes Care 2003;26:1258–1264
4. Somlo S, Mundel P. Getting a foothold in nephrotic syndrome. Nat Genet 2000;24:333–335
5. American Diabetes Association. Standards of medical care in diabetes—2011. Diabetes Care 2011;34(Suppl. 1):S11–S61
6. Fioretto P, Caramori ML, Mauer M. The kidney in diabetes: dynamic pathways of injury and repair. The Camillo Golgi Lecture 2007. Diabetologia 2008;51:1347–1355
7. Steinke JM, Mauer M; International Diabetic Nephropathy Study Group. Lessons learned from studies of the natural history of diabetic nephropathy in young type 1 diabetic patients. Pediatr Endocrinol Rev 2008;5(Suppl. 4):958–963
8. Meyer TW, Bennett PH, Nelson RG. Podocyte number predicts long-term urinary albumin excretion in Pima Indians with type II diabetes and microalbuminuria. Diabetologia 1999;42:1341–1344
9. Pagtalunan ME, Miller PL, Jumping-Eagle S, et al. Podocyte loss and progressive glomerular injury in type II diabetes. J Clin Invest 1997;99:342–348
10. Steffes MW, Schmidt D, McCrery R, Basgen JM; International Diabetic Nephropathy Study Group. Glomerular cell number in normal subjects and in type 1 diabetic patients. Kidney Int 2001;59:2104–2113
11. Verzola D, Gandolfo MT, Ferrario F, et al. Apoptosis in the kidneys of patients with type II diabetic nephropathy. Kidney Int 2007;72:1262–1272
12. White KE, Bilous RW, Marshall SM, et al. Podocyte number in normotensive type 1 diabetic patients with albuminuria. Diabetes 2002;51:3083–3089
13. Tejada T, Catanuto P, Ijaz A, et al. Failure to phosphorylate AKT in podocytes from mice with early diabetic nephropathy promotes cell death. Kidney Int 2008;73:1385–1393
14. Fornoni A, Sageshima J, Wei C, et al. Rituximab targets podocytes in recurrent focal segmental glomerulosclerosis. Sci Transl Med 2011;3:85ra46
15. Attie AD. ABCA1: at the nexus of cholesterol, HDL and atherosclerosis. Trends Biochem Sci 2007;32:172–179
16. Willer CJ, Sanna S, Jackson AU, et al. Newly identified loci that influence lipid concentrations and risk of coronary artery disease. Nat Genet 2008; 40:161–169
17. Zhou H, Tan KC, Shiu SW, Wong Y. Cellular cholesterol efflux to serum is impaired in diabetic nephropathy. Diabetes Metab Res Rev 2008;24:617–623
18. Tang C, Kanter JE, Bornfeldt KE, Leboeuf RC, Oram JF. Diabetes reduces the cholesterol exporter ABCA1 in mouse macrophages and kidneys. J Lipid Res 2010;51:1719–1728

19. Wang Z, Jiang T, Li J, et al. Regulation of renal lipid metabolism, lipid accumulation, and glomerulosclerosis in FVBdb/db mice with type 2 diabetes. Diabetes 2005;54:2328–2335
20. Proctor G, Jiang T, Iwahashi M, Wang Z, Li J, Levi M. Regulation of renal fatty acid and cholesterol metabolism, inflammation, and fibrosis in Akita and OVE26 mice with type 1 diabetes. Diabetes 2006;55:2502–2509
21. Schaefer EJ, Santos RD, Asztalos BF. Marked HDL deficiency and premature coronary heart disease. Curr Opin Lipidol 2010;21:289–297
22. Katz A, Udata C, Ott E, et al. Safety, pharmacokinetics, and pharmacodynamics of single doses of LXR-623, a novel liver X-receptor agonist, in healthy participants. J Clin Pharmacol 2009;49:643–649
23. Grefhorst A, Elzinga BM, Voshol PJ, et al. Stimulation of lipogenesis by pharmacological activation of the liver X receptor leads to production of large, triglyceride-rich very low density lipoprotein particles. J Biol Chem 2002;277:34182–34190
24. López CA, de Vries AH, Marrink SJ. Molecular mechanism of cyclodextrin mediated cholesterol extraction. PLOS Comput Biol 2011;7:e1002020
25. Christian AE, Haynes MP, Phillips MC, Rothblat GH. Use of cyclodextrins for manipulating cellular cholesterol content. J Lipid Res 1997;38:2264–2272
26. Stella VJ, He Q. Cyclodextrins. Toxicol Pathol 2008;36:30–42
27. Berthier CC, Zhang H, Schin M, et al. Enhanced expression of Janus kinase-signal transducer and activator of transcription pathway members in human diabetic nephropathy. Diabetes 2009;58:469–477
28. Cohen CD, Frach K, Schlöndorff D, Kretzler M. Quantitative gene expression analysis in renal biopsies: a novel protocol for a high-throughput multicenter application. Kidney Int 2002;61:133–140
29. Lindenmeyer MT, Kretzler M, Boucherot A, et al. Interstitial vascular rarefaction and reduced VEGF-A expression in human diabetic nephropathy. J Am Soc Nephrol 2007;18:1765–1776
30. Johnson WE, Li C, Rabinovic A. Adjusting batch effects in microarray expression data using empirical Bayes methods. Biostatistics 2007;8:118–127
31. Saeed AI, Bhagabati NK, Braisted JC, et al. TM4 microarray software suite. Methods Enzymol 2006;411:134–193
32. Saeed AI, Sharov V, White J, et al. TM4: a free, open-source system for microarray data management and analysis. Biotechniques 2003;34:374–378
33. Saleem MA, O'Hare MJ, Reiser J, et al. A conditionally immortalized human podocyte cell line demonstrating nephrin and podocin expression. J Am Soc Nephrol 2002;13:630–638
34. Kruth HS. Histochemical detection of esterified cholesterol within human atherosclerotic lesions using the fluorescent probe filipin. Atherosclerosis 1984;51:281–292
35. Mendez AJ. Monensin and brefeldin A inhibit high density lipoprotein-mediated cholesterol efflux from cholesterol-enriched cells. Implications for intracellular cholesterol transport. J Biol Chem 1995;270:5891–5900
36. Khera AV, Cuchel M, de la Llera-Moya M, et al. Cholesterol efflux capacity, high-density lipoprotein function, and atherosclerosis. N Engl J Med 2011;364:127–135
37. Mendez AJ. Cholesterol efflux mediated by apolipoproteins is an active cellular process distinct from efflux mediated by passive diffusion. J Lipid Res 1997;38:1807–1821
38. Fornoni A, Pileggi A, Molano RD, et al. Inhibition of c-jun N terminal kinase (JNK) improves functional beta cell mass in human islets and leads to AKT and glycogen synthase kinase-3 (GSK-3) phosphorylation. Diabetologia 2008;51:298–308
39. Ramirez CM, Liv B, Taylor AM, et al. Weekly cyclodextrin administration normalizes cholesterol metabolism in nearly every organ on the Niemann-Pick Type 1C mouse and markedly prolongs life. Pediatric Res 2010;68:309–315
40. Takahashi N, Boysen G, Li F, Li Y, Swenberg JA. Tandem mass spectrometry measurements of creatinine in mouse plasma and urine for determining glomerular filtration rate. Kidney Int 2007;71:266–271
41. Doi T, Striker LJ, Quaife C, et al. Progressive glomerulosclerosis develops in transgenic mice chronically expressing growth hormone and growth hormone releasing factor but not in those expressing insulinlike growth factor-1. Am J Pathol 1988;131:398–403
42. Van Rooyen DM, Farrell GC. SREBP-2: a link between insulin resistance, hepatic cholesterol, and inflammation in NASH. J Gastroenterol Hepatol 2011;26:789–792
43. Hudkins KL, Pichaiwong W, Wietecha T, et al. BTBR Ob/Ob mutant mice model progressive diabetic nephropathy. J Am Soc Nephrol 2010;21:1533–1542
44. Diez-Sampedro A, Lenz O, Fornoni A. Podocytopathy in diabetes: a metabolic and endocrine disorder. Am J Kidney Dis 2011;58:637–646
45. Helfand BT, Mendez MG, Murthy SN, et al. Vimentin organization modulates the formation of lamellipodia. Mol Biol Cell 2011;22:1274–1289
46. Fackler OT, Grosse R. Cell motility through plasma membrane blebbing. J Cell Biol 2008;181:879–884
47. Coleman ML, Sahai EA, Yeo M, Bosch M, Dewar A, Olson MF. Membrane blebbing during apoptosis results from caspase-mediated activation of ROCK I. Nat Cell Biol 2001;3:339–345
48. Sebbagh M, Renvoizé C, Hamelin J, Riché N, Bertoglio J, Bréard J. Caspase-3-mediated cleavage of ROCK I induces MLC phosphorylation and apoptotic membrane blebbing. Nat Cell Biol 2001;3:346–352
49. Qi M, Liu Y, Freeman MR, Solomon KR. Cholesterol-regulated stress fiber formation. J Cell Biochem 2009;106:1031–1040
50. Zador IZ, Deshmukh GD, Kunkel R, Johnson K, Radin NS, Shayman JA. A role for glycosphingolipid accumulation in the renal hypertrophy of streptozotocin-induced diabetes mellitus. J Clin Invest 1993;91:797–803
51. Xie X, Brown MS, Shelton JM, Richardson JA, Goldstein JL, Liang G. Amino acid substitution in NPC1 that abolishes cholesterol binding reproduces phenotype of complete NPC1 deficiency in mice. Proc Natl Acad Sci USA 2011;108:15330–15335
52. Tam J, Cinar R, Liu J, et al. Peripheral cannabinoid-1 receptor inverse agonism reduces obesity by reversing leptin resistance. Cell Metab 2012;16:167–179
53. Maggio AB, Mueller P, Wacker J, et al. Increased pancreatic fat fraction is present in obese adolescents with metabolic syndrome. J Pediatr Gastroenterol Nutr 2012;54:720–726
54. Kruit JK, Wijesekara N, Westwell-Roper C, et al. Loss of both ABCA1 and ABCG1 results in increased disturbances in islet sterol homeostasis, inflammation, and impaired β-cell function. Diabetes 2012;61:659–664
55. Wijesekara N, Zhang LH, Kang MH, et al. miR-33a modulates ABCA1 expression, cholesterol accumulation, and insulin secretion in pancreatic islets. Diabetes 2012;61:653–658
56. Schwartz GG, Olsson AG, Abt M, et al.; dal-OUTCOMES Investigators. Effects of dalcetrapib in patients with a recent acute coronary syndrome. N Engl J Med 2012;367:2089–2099